CDKN2A (p16[INK4A]) affects the anti-tumor effect of CDK inhibitor in somatotroph adenomas

YIYUAN CHEN[1,2], ZHENYE LI[2], QIUYUE FANG[1,2], HONGYUN WANG[1],
CHUZHONG LI[1-4], HUA GAO[1] and YAZHUO ZHANG[1-4]

[1]Department of Cell Biology, Beijing Neurosurgical Institute, Capital Medical University; [2]Department of Neurosurgery, Beijing Tiantan Hospital Affiliated to Capital Medical University; [3]Department of Cell Biology, China National Clinical Research Center for Neurological Diseases, Beijing Tiantan Hospital, Capital Medical University; [4]Department of Cell Biology, Brain Tumor Center, Beijing Institute for Brain Disorders, Beijing 100070, P.R. China

Abstract. The altered cell cycle is associated with aberrant growth factor signaling in somatotroph adenoma, which is the primary cause of acromegaly. The aim of the present study was to investigate the pathological role of the INK4 family and evaluate the effectiveness of *CDK4* inhibitor, palbociclib, in somatotroph adenoma. RNA-Seq, RT-PCR, and immunohistochemistry were applied to measure the levels and correlations of the INK4 family with angiogenesis, CDKs, EMT, and therapeutic targets. MTS, flow cytometry, and ELISA were used to investigate the bio-activity in GH3 and GT1-1 cell lines after palbociclib treatment. Compared with lactotroph adenoma, gonadotroph adenoma, and corticotroph adenoma, somatotroph samples demonstrated higher expression of *CDKN2A* and *SSTR2* but a lower expression of *EGFR*, *CDK4*, and *CDH2* (P<0.05). *CDKN2A* positively correlates with *SSTR2*, and negatively with *CDK4*, *EGFR*, and *CDH2*. Patients with lower *CDKN2A* had larger tumor size (P=0.016) and more invasive potential (P=0.023). Palbociclib inhibited cell proliferation, induced G1 phase arrest, reduced *GH/IGF-1* secretion of GH3 and GT1-1 cell lines (P<0.05), and had a more prominent role in GH3 cells (P<0.05). *CDKN2A* inhibited the bio-activity by modulating *CDK4*, and high *CDKN2A* predicted the insensitivity to *CDK4* inhibitor, palbociclib, in somatotroph adenoma patients. In summary, the present study shows *CDKN2A* inhibited the bio-activity by modulating *CDK4*, and high *CDKN2A* predicts the insensitivity to *CDK4* inhibitor, Palbociclib, in somatotroph adenoma patients.

Correspondence to: Dr Yazhuo Zhang, Department of Cell Biology, Beijing Neurosurgical Institute, Capital Medical University, 119 South Fourth Ring, Beijing 100070, P.R. China
E-mail: zyz2004520@yeah.net

Introduction

Pituitary neuroendocrine tumors (PitNETs) have five main histological subtypes: somatotroph, lactotroph, thyrotroph, corticotroph, and gonadotroph (1). Somatotroph adenomas (SOMA) are the primary cause of acromegaly, leading to severe complications such as hypertension, diabetes mellitus, cardiovascular disease, osteoarthritis, and sleep apnea (2). Transsphenoidal surgery is the first choice for patients with somatotrophic adenoma. For failed surgery, poor surgical candidates, or residual tumors, drug therapy is used as adjuvant treatment (3). However, the normalization of serum growth hormone/insulin-like growth factor 1 (*GH/IGF-1*) in patients treated with octreotide and lanreotide for one year was 43% and 31-35%, respectively (4,5). An international, non-interventional multicenter study of 2,090 patients with pegvisomant proved that the patient's ratio with normal *IGF-1* increased from 53% at 1 year to 73% at 10 years. However, most patients (72.2%) had no change in tumor size relative to the prior scan, and 22% of patients had severe adverse events (6). Thus, it is imperative to find new mechanisms and molecular for the medical treatment of SOMA.

Cell cycle dysregulation results in uncontrolled proliferation in cancers, including lung cancer, hepatic carcinoma, leukemia, and gynecologic oncology (7). Cyclin-dependent kinases (CDK) are a family of protein kinases involved in

regulating the cycle of mammalian cell division, which in turn is limited by CDK inhibitors (CKIs) (8,9). The cell cycle is negatively regulated by CKIs (8,10), which includes Cip/Kip and INK4 family (11). Somatotroph cells are usually characterized by aneuploidy, DNA damage, and cell cycle disruption, including premature cell cycle arrest (12). Overexpression of cyclin E/*CDK2* and loss of p21^CIP1/p27^KIP1 appeared to be associated with poor prognosis in SOMA (13). The INK4 family shares similar domains that competes with Cyclin D and relieves the activation of *CDK4/6* (14), leading to cell cycle arrest in the G1/S phase (15). Loss of cyclin-dependent kinase inhibitor 2A (*CDKN2A*) predicted sensitivity to the *CDK4/6* inhibitor, PD0332991, in melanoma cell lines (16). *CDKN2A* specifically prevented both nucleotide probe and palbociclib binding to *CDK4* in MCF7 cell line (14).

At present, the pathogenesis of SOMA has not been well elucidated. However, disruption of the cell cycle is considered to play an essential role in pituitary tumorigenesis. The aim of the present study was to describe the characteristic profile of the INK4 family in SOMA, which was different from that of other subtype adenomas and further analyze the correlation of INK4 family with angiogenesis, CDKs activity, epithelial-mesenchymal transition (EMT) and the therapeutic target of SOMA. Based on these results, we hope to provide the evidence of combined the *CDK4/6* inhibitor for the medical treatment of SOMA.

Materials and methods

Patients and samples. Tumor specimens were collected at Beijing Tiantan Hospital affiliated to Capital Medical University from May 2012 through December 2017 after transsphenoidal surgery. Isolated specimens were stored in liquid nitrogen for 30-60 min. All patients had sporadic adenomas and had no family history of adenomas. The morpho-functional classification of pituitary adenomas was diagnosed according to the 2017 World Health Organization (WHO) classification of tumors of endocrine organs (17). The patients comprised 112 (56.6%) males and 86 (43.4%) females with the average age of 46.3±13.5 years (range, 21-69). The study protocol was approved by the Internal Review Board of Beijing Tiantan Hospital Affiliated to Capital Medical University, and conformed to the ethical guidelines laid down in the Declaration of Helsinki (no. KY-2013-015-02). Knosp classification was based on coronal sections of unenhanced and gadolinium diethylene-triamine-pentaacetic acid enhanced magnetic resonance imaging scans, with the readily detectable internal carotid artery serving as the radiological landmark. Surgically proven invasion of the cavernous sinus space was present in all Grade 4 and Grade 3 cases and in all but one of the Grade 2 cases; no invasion was present in Grade 0 and Grade 1 cases (18). All the samples were obtained after informed consent of patients, following institutional review board-approved protocols. Three normal pituitary samples were obtained from the Tianjin Red Cross Society by autopsy through the human body donation program.

GH3 and GT1-1 cell lines were purchased from ATCC (Manassas) and cultured in a humidified incubator at 37°C and 5% CO_2 in F-12K medium (ATCC), supplemented with 2.5% fetal bovine serum and 10% horse serum (Gibco).

RNA extractions, sequencing, RNA-Seq data processing and analysis. For RNA extractions, patient samples were assessed with AllPrep DNA/RNA Mini kit (Qiagen) according to the manufacturer's instructions. The quantity and quality of RNA was evaluated by RNA Nano6000 assay kit (Aligent Technologies) (RIN >6.8). Then, 3 μg RNA/sample was used for RNA preparations, and the ribosomal RNA was removed by Epicentre Ribo-zero™ rRNA Removal kit (Epicentre). Sequencing library was generated by NEBNext® UltraTM Directional RNA Library Prep kit (NEB). The library fragments (150-200 bp) were purified by AMPure XP system (Beckman Coulter), and assessed by Agilent Bioanalyzer 2100 system. The libraries were sequenced on an Illumina Hiseq X platform, then 150 bp paired-end reads were generated. Any reads containing adapters, containing ploy-N and low-quality reads were removed. Clean reads were mapped to the human reference genome (NCBI37/hg19) using hisat2 (v2.0.5) to get reads counts/FPKM/TPM for each identified gene. RStudio was used to analyze the correlation coefficient and significative degree. R package ggplot2 (https://github.com/tidyverse/ggplot2) was used to visualize the results.

Reverse transcription-quantitative polymerase chain reaction (RT-qPCR) analysis. Total RNA of 32 samples was extracted and purified using the RNeasy®Mini kit (QiaGen), following the manufacturer's instructions. Reverse transcriptase kit was used (Applied biosystems, Thermo Fisher Scientific, Inc.), and Quantitative real-time PCR (RT-qPCR) was performed on QuantStudio5 applied (Thermo Fisher Scientific, Inc.) using Power SYBR®-Green PCR Master Mix (Life Technologies). The mRNA level of crucial genes of angiogenesis, CDKs, EMT, and therapeutic targets of SOMA were measured in this study. The fold-change in differential expression for each gene was calculated using the comparative CT method ($2^{-\Delta\Delta Cq}$ method) in R package with 'PCR' functions (https://github.com/MahShaaban/pcr) (19). GAPDH was used as the reference gene (20).

Tissue microarray construction and immunohistochemistry staining. A total of 198 formalin-fixed (4%, room temperature) paraffin-embedded tissue blocks were sectioned. Three core biopsies (2.0 mm in diameter) were selected from the paraffin-embedded tissue. The cores were transferred to tissue microarrays using a semi-automated system (Aphelys MiniCore). The microarrays were cut into 4-μm sections and incubated with anti-p16^INK4A (rabbit monoclonal, 1:1,000, ab108349, Abcam), anti-*CDH2* (rabbit polyclonal, 1:300, ab18203), anti-*CDK4* (rabbit polyclonal, 1:300, ab137675, Abcam), anti-*EGFR* (rabbit monoclonal, 1:200, ab52894), and anti-*SSTR2* (rabbit monoclonal, 1:400, ab134152) primary antibodies. IHC staining was evaluated in normal pituitary and PitNETs tissue concerning the pattern of expression either cytoplasmic, membranous or nucleus. H-score was also calculated for *CDKN2A/CDH2/CDK4/EGFR/SSTR2* using the intensity and percentage of positive cells. The intensity score (0-3) was multiplied by the percentage of cells that stained with each level of intensity and the sum of these mathematical products was expressed as a score of 0-300. H score

formula was calculated as: Strong intensity (3) x percentage + moderate intensity (2) x percentage + mild intensity (1) x percentage.

Cell viability and cell cycle. GH3 and GT1-1 cells were adjusted to a density of $1x10^5$ cells/ml. A total of 100 μl of the cell suspension was plated into each well of a 96-well plate and cultured overnight with 37°C thermostatic. After palbociclib treatment (1, 5 or 20 μM) for 24, 48 and 72 h, 20 μl of 3-(4,5-diethylthiazol-2-yl)-5-(3-carboxymethoxyphenyl)-2-(4-sulfophenyl)-2H-tetrazolium, inner salt (MTS) solution was added to each well, and the cultures were further incubated for 4 h, 37°C. Absorbance was measured at 490 nm using an ELISA plate reader (Thermo Fisher Scientific, Inc.). After 72 h treatment, the cell cycle was determined with PI Detection kit (Roche Diagnostics) by flow cytometry. Experiments were performed in triplicate.

Enzyme-linked immunosorbent assay. The levels of GH and IGF-1 in cell culture supernatant were measured by ELISA (DE3058-96T, DE2096-96T, Applygen), according to the manufacturer's protocol. A total of 10 μl of supernatant was used per well. Absorbance was read at 450 nm using an ELISA plate reader (Thermo Fisher Scientific, Inc.). Experiments were performed in triplicate.

SDS-PAGE and western blot analysis. Samples (up to 10 mg) were lysed in lysis buffer containing 1% Nonidet P-40 (Calbiochem, Merk) and protease and phosphatase inhibitor cocktails (Roche) overnight at 4°C. Total extracts were centrifuged at 12,000 x g for 30 min at 4°C, and protein concentration was determined with the BCA method (Pierce Biotechnology). A total of 40 μg of protein per lane was loaded onto 10% Bis-Tris SDS-PAGE gels, separated electrophoretically, and blotted onto polyvinylidene fluoride membranes (Merk). The blots were incubated with antibodies against anti-p16[INK4A] antibody (1:1,000), anti-*CDK4* antibody (1:2,000), anti-*EGFR* antibody (1:1,000) and anti-*CDH2* antibody (1:1,000) followed by a secondary antibody (1:10,000) tagged with horseradish peroxidase (Santa Cruz Biotechnology). Blots were visualized by enhanced chemiluminescence, and densitometry was performed using a fluorescence image analyzer (Amersham Imager 600, GE Healthcare). *GAPDH* was used as a loading control.

Statistical analysis. Chi test and Fisher's exact test were used to determine the significance of categorical variables. One-way ANOVA (Tukey post-hoc test) and t-test (unpaired test) were applied in patients or for *in vitro* experiments. Spearman correlation coefficient was used for the relationship of INK4 family and crucial genes of angiogenesis, CDKs, EMT, and therapeutic targets of SOMA. P-values were two-sided, and 0.05 was applied as the significance level.

Results

Clinical characteristics of patients. The 198 patients with PitNETs included 38 (19.2%) corticotroph adenomas (CORT), 80 (40.4%) gonadotroph adenomas (GONA), 40 (20.2%) lactotroph adenomas (LACT), 40 (20.2%) SOMA

Table I. Clinical characteristics of 198 pituitary adenoma patients.

Variable	Number	Percentage
Sex		
Male	112	56.57
Female	86	43.43
Age (year)		
Range	21-69	
Mean	46.3±13.5	
Tumor size		
Micro	9	4.54
Macro	127	64.14
Giant	62	31.32
Invasive		
Yes	94	47.47
No	104	52.53
Surgical extent		
Total resection	137	69.19
Partial resection	61	30.81
Recurrence		
Yes	56	28.28
No	142	71.72
Subtypes[a]		
CORT	38	19.2
GONA	80	40.4
LACT	40	20.2
SOMA	40	20.2

[a]CORT, corticotroph PitNETs; GONA, gonadotroph PitNETs; LACT, lactotroph PitNETs; SOMA, somatotroph PitNETs.

and the clinical characteristics are shown in Table I. The patients comprised 112 (56.6%) males and 86 (43.4%) females with the average age of 46.3±13.5 years (range, 21-69). The distribution of tumor volume classifications was 9 (4.54%) microadenomas (diameter ≤1 cm), 127 (64.14%) macroadenomas (1 cm< diameter ≤4 cm), and 62 (31.32%) giant adenomas (diameter >4 cm). According to Knosp staging, there were 94 (47.47%) invasive cases and 104 (52.53%) non-invasive cases. The average follow-up time was 45.5±10.2 months (range, 23-78), and 5-year recurrence rate was 56/198 (28.28%).

Characteristic profile of the INK4 family in SOMA. A total of 24 SOMA specimens were sequenced to obtain the transcriptome reading data after matching, then normalized them to transcripts per million (TPM) values. With these data, the mRNA levels correlation of INK4 family members with crucial genes of angiogenesis, CDKs, EMT, and therapeutic targets of SOMA were analyzed in Fig. 1. Among them, Spearman correlation coefficient of *CDKN2A* and epidermal growth factor receptor (*EGFR*) (r=-0.534, P=0.032), Cadherin 2 (*CDH2*) (r=-0.631, P=0.001), *CDK4* (r=-0.441, P=0.032), Snail family transcriptional repressor 1 (*SNAI1*) (r=0.657, P=0.001),
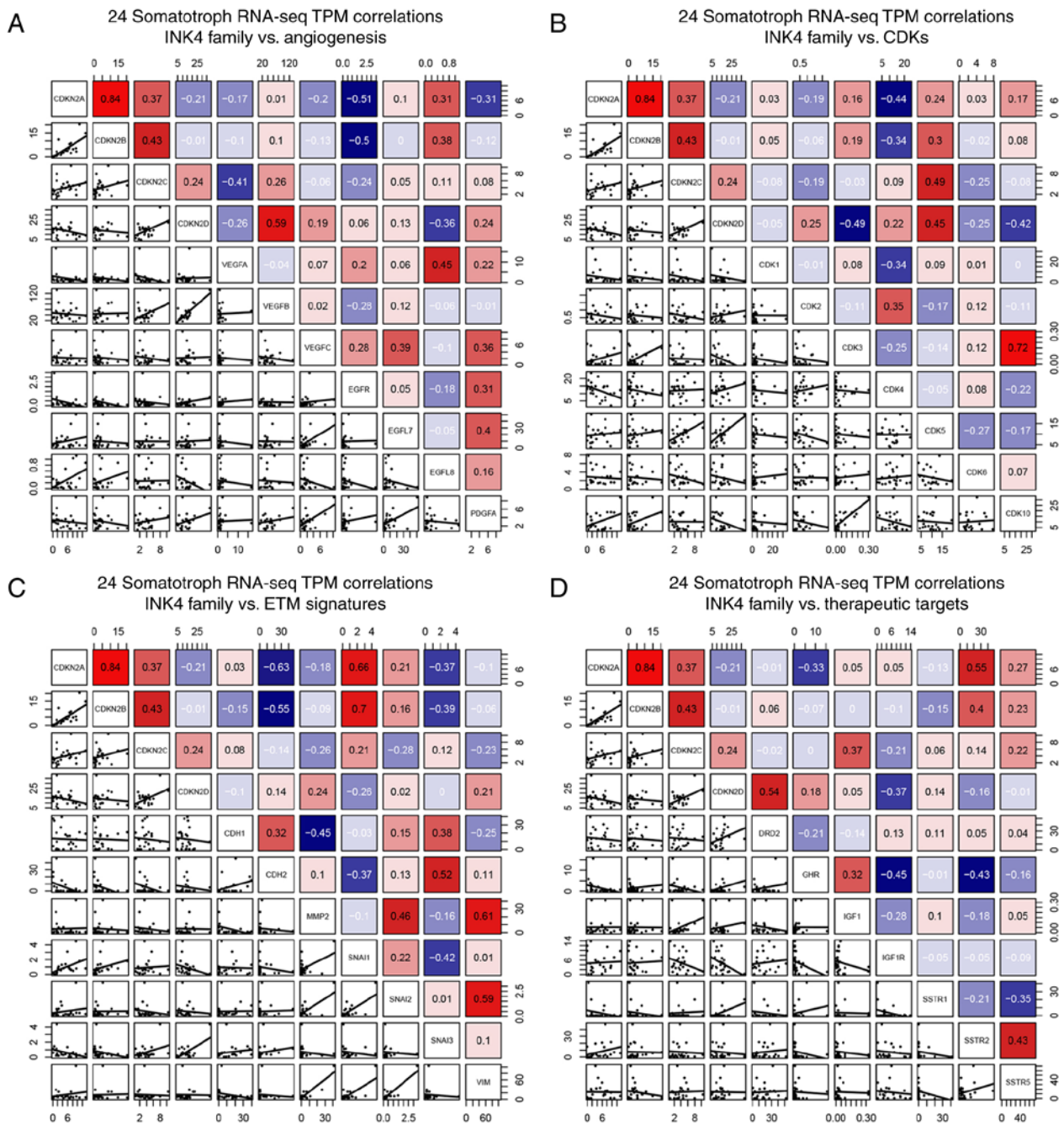
Figure 1. Correlation analyzes of INK4 family with tumor functions by 24 SOMA RNA-Seq TPM data. (A) Angiogenesis. The most negative gene was *EGFR*. (B) CDKs family. The most negative gene was *CDK4*, and the most positive gene was *CDK5*. (C) EMT. The most negative gene was *CDH2*, and the most positive was *SNAI1*. (D) Therapeutic targets of SOMA. The most negative gene was *GHR*, the most positive gene was *SSTR2*.

Somatostatin receptor 2 (*SSTR2*) (r=-0.555, P=0.006) as well as *CDKN2B* and *EGFR* (r=-0.497, P=0.014), *CDH2* (r=-0.545, P=0.007), *SNAI1* (r=0.70, P=0.001); *CDKN2D* and *CDK5* (r=0.45, P=0.029), Dopamine receptor D2 (*DRD2*) (r=0.541, P=0.007) had reached the significance level as shown in Fig. 2A. According to the results, EGFR, *CDK4*, *CDH2*, and *SSTR2* were filtered for the next step.

Subsequently, we analyzed the mRNA levels of the INK4 family and candidate molecules in SOMA, LACT, GONA, and CORT in Fig. 2B via reverse transcriptase-quantitative polymerase chain reaction (RT-qPCR). The levels of *CDKN2A* and *CDKN2B* in SOMA were the highest compared to other subtypes (P<0.01), and the levels of *EGFR* and *CDK4* in SOMA

were the lowest (P<0.05). There was no statistical difference of *CDKN2C* or *CDKN2D* among these subtypes (P>0.05). Based on these results, we chose *CDKN2A* for further research.

Expression profile of CDKN2A in 198 patients by tissue microarray analysis. Protein levels of *CDKN2A*, *EGFR*, *CDK4*, *CDH2*, and *SSTR2* were studied in 198 specimens by immunohistochemistry (IHC) (Fig. 3). Among the five groups, SOMA had the lowest H-score compared to *CDK4*, *CDH2*, and *EGFR*, but had a higher H-score compared to *CDKN2A* and *SSTR2* (P<0.01). Patients were divided into high and low groups based on the median H-score. Patients with lower *CDKN2A* had larger tumor size (58/99 vs. 41/99, P=0.016) and
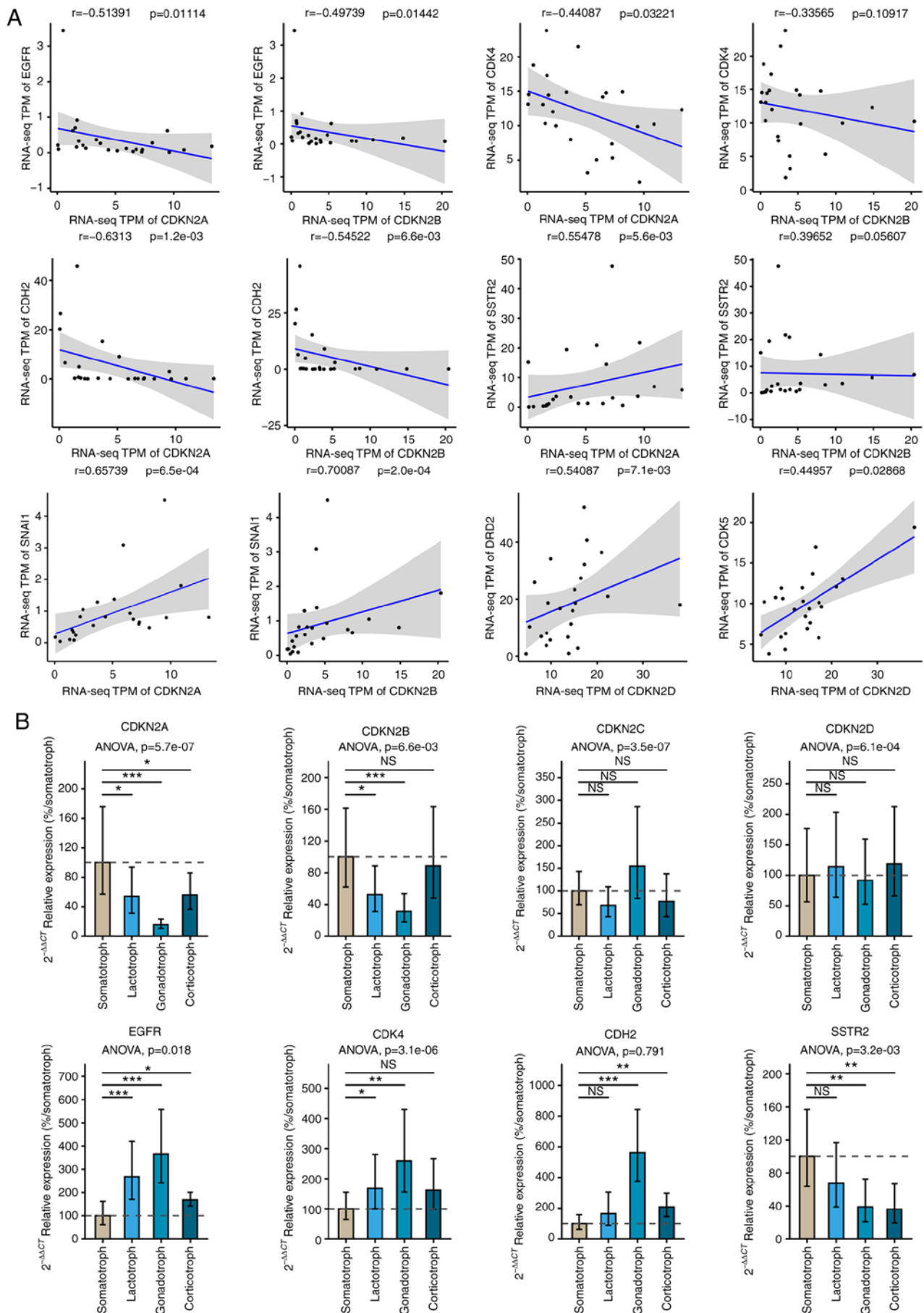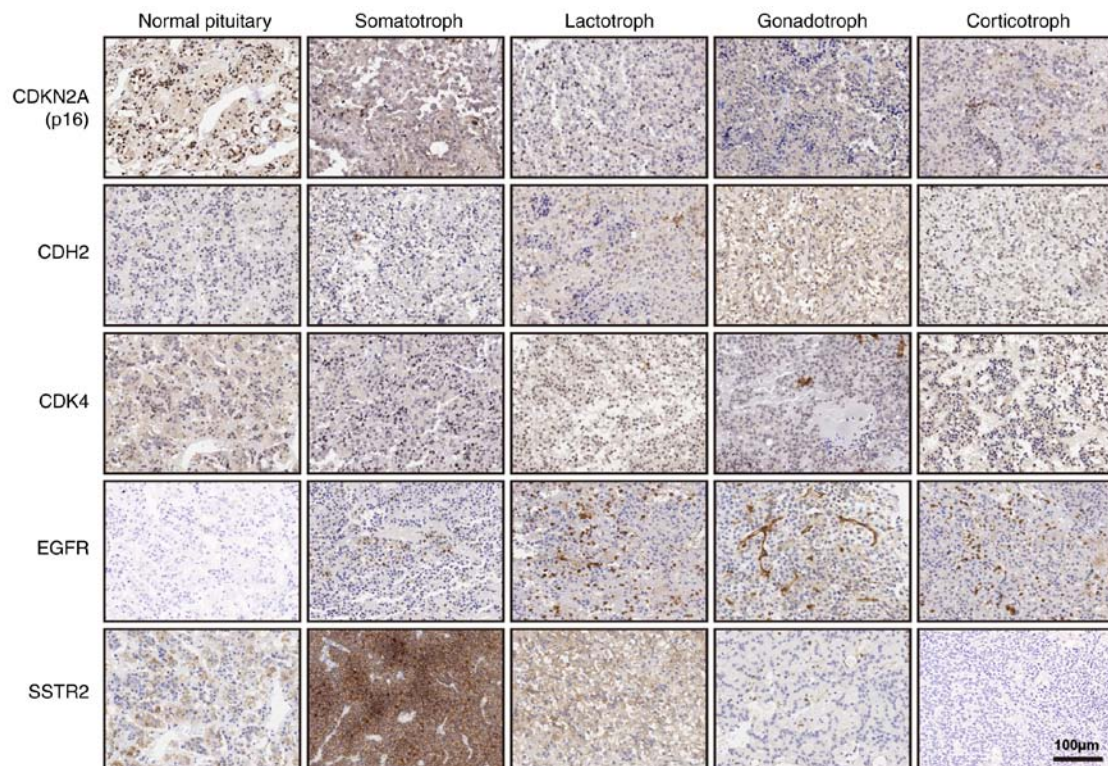
Figure 2. The characteristic profile of the INK4 family in pituitary adenoma. (A) Correlation analysis among INK4 family with the characteristic molecule related to tumor behavior. (B) The mRNA level of INK4 family and characteristic molecule related to tumor behavior in subtypes of pituitary adenomas. *P<0.05, **P<0.01, ***P<0.001, n=8.

Table II. Relationship between CDKN2A, CDKN2C, CDKN2D and various clinical parameters in 198 pituitary adenoma patients.

Variable	CDKN2A			CDKN2C			CDKN2D		
	High	Low	P-value	High	Low	P-value	High	Low	P-value
Sex			P=0.086			P=0.774			P=0.251
Male	50	62		57	55		60	52	
Female	49	37		42	44		39	47	
Age			P=0.065			P=0.320			P=0.118
≤46.3	43	56		46	53		55	44	
>46.3	56	43		53	46		44	55	
Tumor size (cm^3)			P=0.016			P=0.201			P=0.033
≤17.57	41	58		45	54		57	42	
>17.57	58	41		54	45		42	57	
Invasion			P=0.023			P=0.090			P=0.046
Yes	39	55		42	52		54	40	
No	60	44		57	47		45	59	
Resection			P=0.045			P=0.644			P=0.090
Total	75	62		67	70		63	74	
Partial	24	37		32	29		26	25	
Recurrence			P=0.115			P=0.528			P=0.058
Yes	23	33		30	26		34	22	
No	76	66		69	73		65	77	

Figure 3. Immunohistochemistry of *CDKN2A*, *CDH2*, *CDK4*, *EGFR* and *SSTR2* in pituitary and pituitary adenomas. Magnification, x100; bar=100 µm.

higher invasive behavior (55/99 vs. 39/99, P=0.023) (Table II). There was also a negative correlation between *CDKN2A* and invasive behavior (r=-0.207, P=0.0004). Higher *CDK4* might cause more invasive potential (54/99 vs. 40/99, P=0.046). Positive staining of *SSTR2* was 25/80 (31.3%) in GONA. The average H-scores of *SSTR2* were 57.9±20.6 in *SSTR2*+GONA
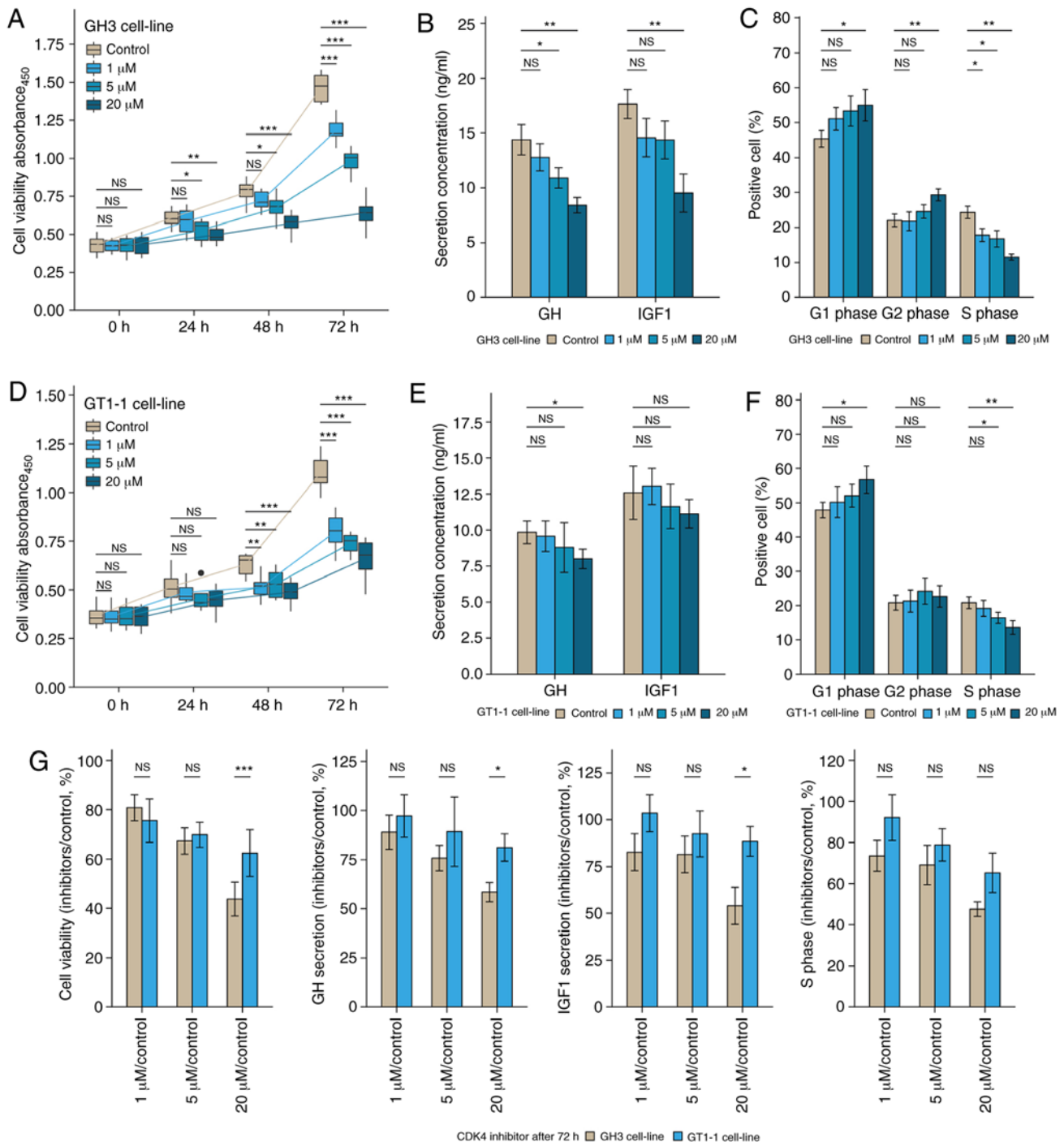
Figure 4. The bio-activity effect of *CDK4/6* inhibitor, Palbociclib, of GH3 and GT1-1 cell line in various concentrations (1, 5, and 20μM). (A and D) The inhibition induced by Palbociclib occurred in a time- and dose-dependent manner, whether GH3 or GT1-1 cells. *P<0.05, **P<0.01, ***P<0.001, n=8. (B and E) Palbociclib inhibited the secretion of *GH/IGF-1* in GH3 and GT1-1 cell lines. (C and F) Palbociclib induced the G1 phase arrest in GH3 and GT1-1 cell lines. (G) Statistical analysis of the change of bio-activity after 72 h treatment between GH3 and GT1-1 cell lines, compared to the control group (%). *P<0.05, **P<0.01, ***P<0.001, n=3.

compared to 143.4±9.17 in SOMA. In addition, we analyzed the correlation of *DRD2* and *CDKN2A* in 40 SOMA patients and 4 normal pituitary samples by IHC experiment. H-scores of *DRD2* in SOMA were 160.1±7.2 (range: 50-270), and 195±25.69 (160, 210, 210 and 270) in normal pituitary. Correlation coefficient was 0.22 (P=0.151) in Fig. S1.

Inhibition induced by palbociclib in GH3 and GT1-1 cell line. The bioactivity effect of *CDK4/6* inhibitor, palbociclib,

was tested on the GH3 and GT1-1 cell lines. The cell viability experiment showed that inhibition by palbociclib occurred in a dose- and time-dependent manner (Fig. 4A and D). Levels of *GH/IGF-1* in cell culture supernatant declined in a dose-dependent manner after 72 h treatment in Fig. 4B and E. Flow cytometry showed that Palbociclib induced G1 phase arrest, whether in GH3 or GT1-1 cells (Figs. 4C and F, S2). It was reported that the level of *CDKN2A* was correlated with the sensitivity of *CDK4* inhibitor, palbociclib. Statistical analysis
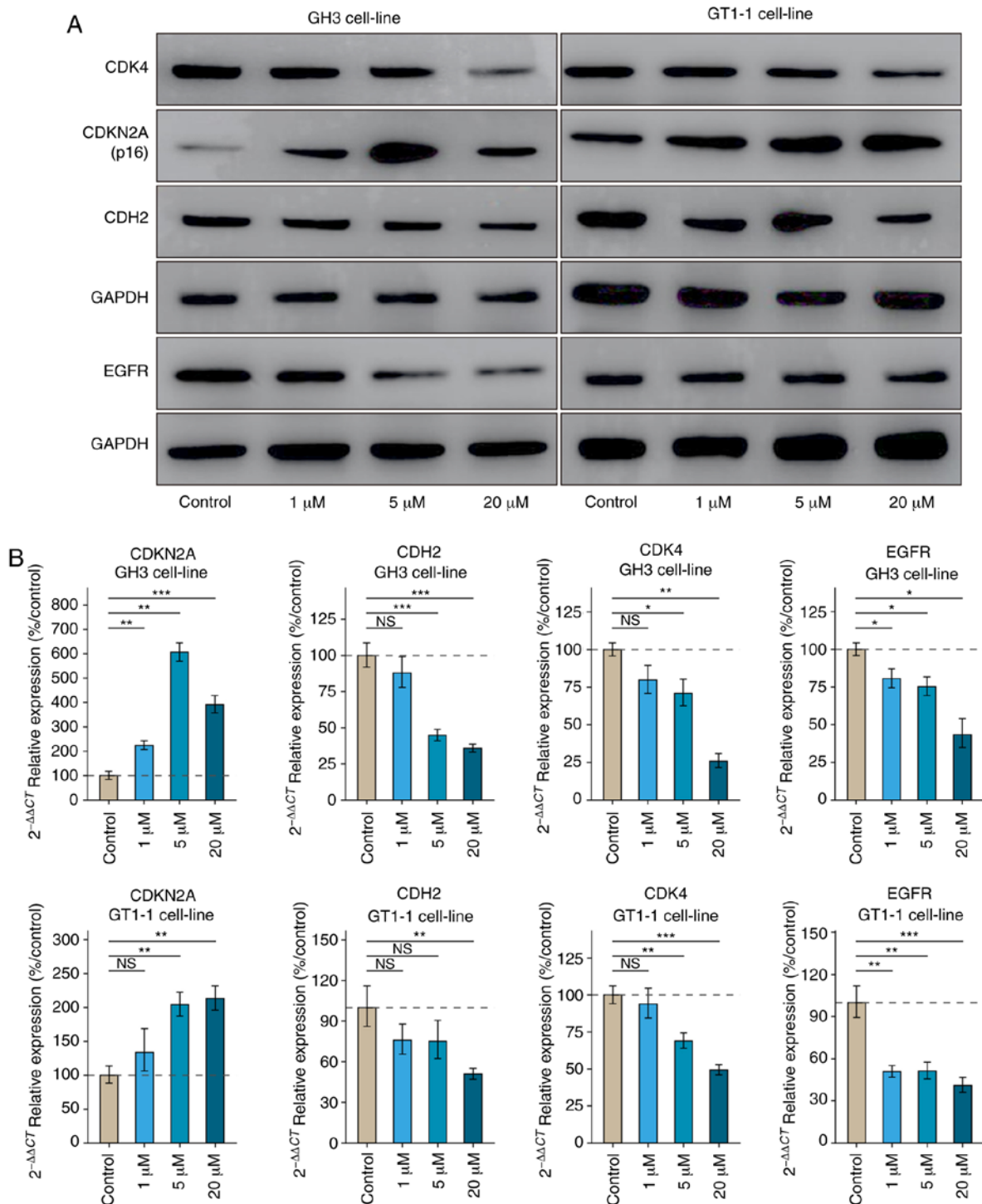
Figure 5. Palbociclib relieved the levels of *CDH2*, *CDK4* and *EGFR* accompanied by upregulation of *CDKN2A* in various concentrations (1, 5, and 20 μM). (A) Bands of western blot assay. (B) Statistical analysis of mRNA level in RT-qPCR assay. compared to control group. *P<0.05, **P<0.01, ***P<0.001, n=3.

of cell viability, and secretion of *GH/IGF-1* both showed the inhibition of palbociclib in the GH3 cell line was stronger than that in the GT1-1 cell line after 72 h treatment (Fig. 4G) (P<0.05).

Results of the RT-qPCR and western blot assays showed palbociclib undermined the level of *CDK4*, *CDH2*, and *EGFR* (Fig. 5). Western blot analysis revealed that the level of *CDKN2A* in GH3 cells was lower than that in GT1-1 cells. Palbociclib has more potent inhibition on the activity of *CDK4* in GH3 cell line than in GT1-1 cell line.

Discussion

SOMA accounts for 13-15% of functional PitNETs and are more common in males with a high standardized mortality ratio compared with the general population (21). Factors associated with successful treatment include tumor size, preoperative serum *GH/IGF-1* level, and parasellar extension (22). Disruption of cell cycle played a crucial role in pituitary tumorigenesis. Classifying the relationship of cell cycle involving SOMA biology may provide new therapeutic

molecule against SOMA. Herein, we described the profile of INK4 family in SOMA. The level of *CDKN2A* should be evaluated for the strategy combined with CKIs in future medical treatment.

Excess proliferation and gene dysregulation are the hallmarks of cancer. Checkpoints block cells from passing into the next phase, and CDKs control critical cell cycle checkpoints and key transcriptional events. The first checkpoint occurs at the G1-S phase, and the G1-S enzymes include *CDK4*, *CDK6*, and the D-type cyclins (23). The INK4 family regulates the G1-to-S phase transition by specifically inhibiting the activity of *CDK4/6*. *CDKN2A/CDKN2B* have unique structures and are essential tumor suppressor genes; loss of *CDKN2A* function was correlated with an increased risk of pancreatic cancer (24-26). In addition, low level or loss of *CDKN2A* was associated with shorter disease-free survival and disease-specific survival times, independent of tumor size and WHO grade of pancreatic neuroendocrine tumors (27). In this study, patients with low *CDKN2A* had larger tumor volume and a higher likelihood of invasive behavior than patients with high *CDKN2A*. Correlation analysis of mRNA levels was measured in *CDKN2A* and CDKs. *CDK4* was filtered as the regulatory protein of *CDKN2A*. The negative correlation between *CDKN2A* and *CDH2* was identified. *CDH2* knockdown markedly inhibited cell proliferation, colony formation, cell migration and invasion, and induced cell cycle arrest and apoptosis (28).

The ankyrin-repeat protein *CDKN2D* functions as a key regulator of G1/S transition, and phosphorylation of *CDKN2D* dissociates the *CDK6-CDKN2D* inhibitory complex, thereby, activating *CDK6*, which triggers entry into S-phase (29). Considering the dual role of *CDKN2D* in controlling differentiation and proliferation (30), the positive correlation between *CDKN2D* and *CDK5* was not significant in SOMA. *CDKN2A* and *CDKN2D* played a converse role in the tumor proliferation and invasion of SOMA heeding the relationship with genes related to EMT, at least, albeit *CDKN2D* was not an inhibitor of *CDK4* activity in SOMA.

Recent evidence indicates epithelial-mesenchymal transition (EMT) plays a critical role in stemness, metabolic reprogramming, immune evasion and therapeutic resistance of cancer cells. Transcriptional repressors including Snail (*SNAI1*), Slug (*SNAI2*) and the ZEB family constitute key players for EMT in cancer as well as in the developmental process (31). However, Tamura *et al* reported that the expression of SNAIL1 was significantly associated with suprasellar expansion, which was not related to tumor invasion (32). Jia *et al* reported that *SNAI1* had a significant correlation of PitNET proliferation, and *SNAI2* had a significant correlation of sella destruction (33). In summary, the bio-activity of *SNAI1* in PitNETs should be investigated to clarify its role further in future research. Therefore, we chose the most significant molecule, *CDH2*, which is related to EMT. RT-qPCR and IHC experiments both indicated the negative correlation between *CDKN2A* and *CDH2*.

CDK4/6 was known to promote continued cell-cycle progression and growth in cancer. The imbalance of *CDK4/6* causes resistance to endocrine therapy in hormone receptor-positive breast cancer (34). Palbociclib, combined with the aromatase inhibitor, letrozole, significantly prolonged progression-free survival as compared with letrozole alone in a double-blind study of advanced breast cancer (35). An ovarian patient with loss of *CDKN2A* derived significant, prolonged clinical benefit from Palbociclib with letrozole (36). High *CDKN2A* should be one of the exclusion criteria for *CDK4/6* inhibitor therapy for high *CDK4* target engagement by Palbociclib in cells without functional *CDKN2A* and attenuated target engagement when *CDKN2A* is abundant (14). GH3 cells mainly secrete growth hormone and insulin-like growth factor, and GT1-1 cells mainly secrete luteinizing hormone accompanied with a little growth hormone. Theoretically, *CDKN2A* should be increased with the increase of Palbociclib. However, the level of *CDKN2A* in 20 μM group did not support our hypothesis. We speculated that the dose of Palbociclib (20 μM) was overdosed for the GH3 cell line. In summary, IC50 value of *CDK4/6* inhibitor is 23 nM to 10 μM in several cell lines including MU4-11, MCF7, WM2664, BV173 and H69 (37).

In this study, we identified the lower level of *CDKN2A* in GH3 cell line compared to that in the GT1-1 cell line based on the western blot experiment. Palbociclib showed a more potent inhibition of the level of *CDK4*, cell proliferation, and cell cycle in the GH3 cell line compared to the GT1-1 cell line. There was a negative correlation between *CDKN2A* and *CDK4* in SOMA specimens. Future study aims to examine the RNAi-*CDKN2A* and plasmid overexpression in *in vitro/in vivo* experiments, which can enhance the results of anti-*CDKN2A* antibody blockade in the current study. Palbociclib-combined SSAs should be a potent strategy in SOMA patients with low *CDKN2A* level. Anderson *et al* reported that metastatic breast cancer combined with non-functional adenoma was treated with Palbociclib, and routine imaging demonstrated significant regression of pituitary adenoma after one-year treatment (38).

Furthermore, we found nearly one-third of *SSTR2*-positive cases in GONA, which provided the evidence of 35±13% control ratio in non-functioning pituitary tumors by *SSTR2* agonists (1). Combined with a low level of *CDKN2A* in GONA, Palbociclib-combined SSAs should be evaluated in future clinical trials. Lack of animal experiments and non-availability of biomolecular details were some of the limitations of the current study. For DNA hypomethylation and chromosomal instability in SOMA, the epigenetic signature of the INK4 family should be explored in future research.

In conclusion, correlations between *CDKN2A* and tumor biological behaviors were established in SOMA. Furthermore, nearly one-third of GONA had a positive *SSTR2* expression. *CDKN2A* expression involved the inhibition of cell proliferation and *GH/IGF-1* secretion induced by *CDK4/6* inhibitor, and Palbociclib in *in vitro* experiments. Therefore, we suggest the combination of *CDK4* inhibitor and SSAs, can be used as potential therapeutic candidates for targeting residual SOMA or GONA with high *CDKN2A* expression.

Availability of data and materials

We agree that all datasets on which the conclusions of the manuscript rely to be either deposited in publicly available repositories (where available and appropriate) or presented in the main paper or additional supporting files, in machine-readable format (such as spreadsheets rather than PDFs) whenever possible.

Authors' contributions

YC was involved in IHC experiments and writing the manuscript. ZL was responsible for cell functional experiments. QF conducted the PCR experiments. HW was responsible for performing cell culture and functional experiments. CL carried out RNA-seq and data analysis. HG was involved in data collection and statistical analysis thereof. YZ designed the protocol and revised the manuscript. All authors read and approved the final manuscript.

Ethics approval and consent to participate

Informed consent was obtained from all individuals and ethical approval was obtained from the Institutional Review Board of Beijing Tiantan Hospital Affiliated to Capital Medical University (KY2013-015-02).

Patient consent for publication

All patients signed the informed consent.

Competing interests

The authors declare that they have no competing interests.

References

1. Neou M, Villa C, Armignacco R, Jouinot A, Raffin-Sanson ML, Septier A, Letourneur F, Diry S, Diedisheim M, Izac B, *et al*: Pangenomic classification of pituitary neuroendocrine tumors. Cancer Cell 13: S1535610819305227, 2019.
2. Racine MS and Barkan AL: Medical management of growth hormone-secreting pituitary adenomas. Pituitary 5: 67-76, 2002.
3. Molitch ME: Diagnosis and treatment of pituitary adenomas: A Review. JAMA 317: 516-524, 2017.
4. Melmed S, Popovic V, Bidlingmaier M, Mercado M, van der Lely AJ, Biermasz N, Bolanowski M, Coculescu M, Schopohl J, Racz K, *et al*: Safety and efficacy of oral octreotide in acromegaly: Results of a multicenter phase III trial. J Clin Endocrinol Metab 100: 1699-1708, 2015.
5. Alquraini H, Del Pilar Schneider M, Mirakhur B and Barkan A: Biochemical efficacy of long-acting lanreotide depot/autogel in patients with acromegaly naïve to somatostatin-receptor ligands: Analysis of three multicenter clinical trials. Pituitary 21: 283-289, 2018.
6. Buchfelder M, van der Lely AJ, Biller BM, Webb SM, Brue T, Strasburger CJ, Ghigo E, Camacho-Hubner C, Pan K, Lavenberg J, *et al*: Long-Term treatment with pegvisomant: Observations from 2090 acromegaly patients in ACROSTUDY. Eur J Endocrinol 179: 419-427, 2018.
7. Rouse J and Jackson SP: Interfaces between the detection, signaling, and repair of DNA damage. Science 297: 547-551, 2002.
8. Sherr CJ and Roberts JM: CDK inhibitors: Positive and negative regulators of G1-phase progression. Genes Dev 13: 1501-1512, 1999.
9. Otto T and Sicinski P: Cell cycle proteins as promising targets in cancer therapy. Nat Rev Cancer 17: 93-115, 2017.
10. Roussel MF: The INK4 family of cell cycle inhibitors in cancer. Oncogene 18: 5311-5317, 1999.
11. Besson A, Dowdy SF and Roberts JM: CDK inhibitors: Cell cycle regulators and beyond. Dev Cell 14: 159-169, 2008.
12. Melmed S: Pathogenesis of pituitary tumors. Nat Rev Endocrinol 7: 257-266, 2011.
13. Dong W, Zhu H, Gao H, Shi W, Zhang Y, Wang H, Li C, Song G and Zhang Y: Expression of cyclin E/Cdk2/p27Kip1 in growth hormone adenomas. World Neurosurg 121: e45-e53, 2019.
14. Green JL, Okerberg ES, Sejd J, Palafox M, Monserrat L, Alemayehu S, Wu J, Sykes M, Aban A, Serra V and Nomanbhoy T: Direct CDKN2 modulation of CDK4 alters target engagement of CDK4 inhibitor drugs. Mol Cancer Ther 18: 771-779, 2019.
15. Sun F, Li N, Tong X, Zeng J, He S, Gai T, Bai Y, Liu L, Lu K, Shen J, *et al*: Ara-C induces cell cycle G1/S arrest by inducing upregulation of the INK4 family gene or directly inhibiting the formation of the cell cycle-dependent complex CDK4/cyclin D1. Cell Cycle 18: 2293-2306, 2019.
16. Young RJ, Waldeck K, Martin C, Foo JH, Cameron DP, Kirby L, Do H, Mitchell C, Cullinane C, Liu W, *et al*: Loss of CDKN2A expression is a frequent event in primary invasive melanoma and correlates with sensitivity to the CDK4/6 inhibitor PD0332991 in melanoma cell lines. Pigment Cell Melanoma Res 27: 590-600, 2014.
17. Lloyd R, Osamura R, Klöppel G and Rosai J: (2017) WHO classification of tumours of the endocrine organs, 4th edn. International Agency for Research on Cancer, Lyon.
18. Knosp E, Steiner E, Kitz K and Matula C: Pituitary adenomas with invasion of the cavernous sinus space: A magnetic resonance imaging classification compared with surgical findings. Neurosurgery 33: 610-617, 1993.
19. Livak KJ and Schmittgen TD: Analysis of relative gene expression data using real-time quantitative PCR and the 2(-Delta Delta C(T)) method. Methods 25: 402-408, 2001.
20. Pabinger S, Rödiger S, Kriegner A, Vierlinger K and Weinhäusel A: A survey of tools for the analysis of quantitative PCR (qPCR) data. Biomol Detect Quantif 1: 23-33, 2014.
21. Dekkers OM, Biermasz NR, Pereira M, Romijn JA and Vandenbroucke JP: Mortality in acromegaly: A metaanalysis. J Clin Endocrinol Metab 93: 61-67, 2008.
22. Starke RM, Raper DM, Payne SC, Vance ML, Oldfield EH and Jane JA: Endoscopic vs microsurgical transsphenoidal surgery for acromegaly: Outcomes in a concurrent series of patients using modern criteria for remission. J Clin Endocrinol Metab 98: 3190-3198, 2013.
23. Tigan AS, Bellutti F, Kollmann K, Tebb G and Sexl V: CDK6-A review of the past and a glimpse into the future: From cell-cycle control to transcriptional regulation. Oncogene 35: 3083-3091, 2016.
24. Kim WY and Sharpless NE: The regulation of INK4/ARF in cancer and aging. Cell 127: 265-275, 2006.
25. Tang B, Li Y, Qi G, Yuan S, Wang Z, Yu S, Li B and He S: Clinicopathological significance of CDKN2A promoter hypermethylation frequency with pancreatic cancer. Sci Rep 5: 13563, 2015.
26. Tian X, Azpurua J, Ke Z, Augereau A, Zhang ZD, Vijg J, Gladyshev VN, Gorbunova V and Seluanov A: INK4 locus of the tumor-resistant rodent, the naked mole rat, expresses a functional p15/p16 hybrid isoform. Proc Natl Acad Sci USA 112: 1053-1058, 2015.
27. Roy S, LaFramboise WA, Liu TC, Cao D, Luvison A, Miller C, Lyons MA, O'Sullivan RJ, Zureikat AH, Hogg ME, *et al*: Loss of chromatin-remodeling proteins and/or CDKN2A associates with metastasis of pancreatic neuroendocrine tumors and reduced patient survival times. Gastroenterology 154: 2060-2063, 2018.
28. Da C, Wu K, Yue C, Bai P, Wang R, Wang G, Zhao M, Lv Y and Hou P: N-Cadherin promotes thyroid tumorigenesis through modulating major signaling pathways. Oncotarget 8: 8131-8142, 2017.
29. Kumar A, Gopalswamy M, Wolf A, Brockwell DJ, Hatzfeld M and Balbach J: Phosphorylation-Induced unfolding regulates p19INK4d during the human cell cycle. Proc Natl Acad Sci USA 115: 3344-3349, 2018.
30. Wang Y, Jin W, Jia X, Luo R, Tan Y, Zhu X, Yang X, Wang X and Wang K: Transcriptional repression of CDKN2D by PML/RARα contributes to the altered proliferation and differentiation block of acute promyelocytic leukemia cells. Cell Death Dis 5: e1431, 2014.

31. Cho ES, Kang HE, Kim NH and Yook JI: Therapeutic implications of cancer epithelial-mesenchymal transition (EMT). Arch Pharm Res 42: 14-24, 2019.
32. Tamura R, Ohara K, Morimoto Y, Kosugi K, Oishi Y, Sato M, Yoshida K and Toda M: PITX2 expression in non-functional pituitary neuroendocrine tumor with cavernous sinus invasion. Endocr Pathol 30: 81-89, 2019.
33. Jia W, Zhu J, Martin TA, Jiang A, Sanders AJ and Jiang WG: Epithelial-Mesenchymal transition (EMT) markers in human pituitary adenomas indicate a clinical course. Anticancer Res 35: 2635-2643, 2015.
34. Shapiro GI: Cyclin-Dependent kinase pathways as targets for cancer treatment. J Clin Oncol 24: 1770-1783, 2006.
35. Finn RS, Martin M, Rugo HS, Jones S, Im SA, Gelmon K, Harbeck N, Lipatov ON, Walshe JM, Moulder S, et al: Palbociclib and letrozole in advanced breast cancer. N Engl J Med 375: 1925-1936, 2016.
36. Frisone D, Charrier M, Clement S, Christinat Y, Thouvenin L, Homicsko K, Michielin O, Bodmer A, Chappuis PO, McKee TA and Tsantoulis P: Durable response to palbociclib and letrozole in ovarian cancer with CDKN2A loss. Cancer Biol Ther 21: 197-202, 2020.
37. Bisi JE, Sorrentino JA, Jordan JL, Darr DD, Roberts PJ, Tavares FX and Strum JC: Preclinical development of G1T38: A novel, potent and selective inhibitor of cyclin dependent kinases 4/6 for use as an oral antineoplastic in patients with CDK4/6 sensitive tumors. Oncotarget 8: 42343-42358, 2017.
38. Anderson E, Heller RS, Lechan RM and Heilman CB: Regression of a nonfunctioning pituitary macroadenoma on the CDK4/6 inhibitor palbociclib: Case report. Neurosurg Focus 44: E9, 2018.